PHYSICAL REVIEW C **81**, 014307 (2010)

Competing quasiparticle configurations in ^{163}W

J. Thomson,[1] D. T. Joss,[1,*] E. S. Paul,[1] C. Scholey,[2] J. Simpson,[3] S. Ertürk,[4] L. Bianco,[1,†] B. Cederwall,[5] I. G. Darby,[1,‡] S. Eeckhaudt,[2] M. B. Gómez-Hornillos,[3,§] T. Grahn,[1] P. T. Greenlees,[2] B. Hadinia,[5,∥] P. Jones,[2] R. Julin,[2] S. Juutinen,[2] S. Ketelhut,[2] M. Leino,[2] M. Nyman,[2] D. O'Donnell,[3] R. D. Page,[1] J. Pakarinen,[1] P. Rahkila,[2] N. Rowley,[3,¶] M. Sandzelius,[2,5] P. J. Sapple,[1] J. Sarén,[2] J. Sorri,[2] and J. Uusitalo[2]

[1]*Oliver Lodge Laboratory, University of Liverpool, Liverpool, L69 7ZE, United Kingdom*

[2]*Department of Physics, University of Jyväskylä, FI-40014 Jyväskylä, Finland*

[3]*STFC Daresbury Laboratory, Daresbury, Warrington WA4 4AD, United Kingdom*

[4]*Niğde Üniversitesi, Fen Edebiyat Fakltesi, Fizik Bölümü, 51100 Nigde, Turkey*

[5]*Department of Physics, Royal Institute of Technology, S-10691 Stockholm, Sweden*

(Received 30 October 2009; published 15 January 2010)

Excited states in the neutron-deficient nuclide ^{163}W were investigated using the ^{106}Cd(^{60}Ni,2pn)^{163}W reaction at a beam energy of 270 MeV. The level scheme for ^{163}W was extended significantly with the observation of five new band structures. The yrast band based on a $13/2^+$ isomeric state is extended up to $(57/2^+)$. Two band structures were established on the $7/2^-$ ground state. Quasiparticle configuration assignments for the new band structures were made on the basis of cranked Woods-Saxon shell-model calculations. The results reported in this article suggest that the negative-parity $\nu(f_{7/2}, h_{9/2})$ orbitals are responsible for the first rotational alignment in the yrast band.

DOI: 10.1103/PhysRevC.81.014307 PACS number(s): 21.10.Re, 27.70.+q, 23.20.Lv

I. INTRODUCTION

Understanding the emergence of collectivity in nuclei is a long-standing goal of nuclear physics. Comparisons of level schemes of nuclei over long chains of isotopes or isotones can reveal the evolution from single-particle structures at shell closures to collective behavior as nucleons are added. Recently, the application of selective tagging techniques [1–3] has allowed excited states in the most neutron-deficient W-Os-Pt-Hg nuclei to be observed, in many cases, for the first time [4–7]. In these cases only the most rudimentary information is available at low spin, although this is often enough to reveal changes in structure and collectivity. For example, the $E(4^+)/E(2^+)$ ratio as a function of neutron number is found to change smoothly, but distinctly, over a small range of neutron numbers indicating spherical shapes near $N = 82$ through γ-soft shapes to deformed rotors [8].

Detailed spectroscopy up to high spin can be performed in nuclei a few nucleons heavier than the most neutron-deficient known isotopes. It is then possible to identify the orbitals responsible for the configurations that are observed. This is important since the overall properties of the nucleus are sensitive to the occupation of the core-polarizing orbitals near the Fermi surface. In the $N \geqslant 90$ W isotopes the $i_{13/2}$ neutron orbital dominates the yrast spectra with the lowest energy quasiparticle configurations involving one (odd-A) or two (even-A) $i_{13/2}$ neutrons [9–11]. In ^{164}W Simpson *et al.* [9] observed the yrast band up to high spin ($I^\pi = 28^+$) and established the first band crossing in the yrast band at $\hbar\omega = 0.29$ MeV with a gain in aligned angular momentum, Δi_x, of 11$\hbar$. This was interpreted as the rotational alignment of a pair of $i_{13/2}$ neutrons, which is also established in the heavier isotopes. However, Dracoulis *et al.* [12] reported measurements of the lighter even-even isotope ^{162}W and measured a comparatively lower alignment gain at the first band crossing $\Delta i_x = 6\hbar$. This was attributed to the rotational alignment of an $h_{9/2}$ neutron pair [12]. The nucleus ^{163}W ($N = 89$) therefore occupies a pivotal location in the transitional W isotopes in which the competition between the positive parity $i_{13/2}$ and the negative-parity orbitals to form the first quasiparticle alignment is most pronounced.

The yrast band of ^{163}W was observed previously [12] from $(13/2^+)$ to $(49/2^+)$. Scholey *et al.* established that the $13/2^+$ state is isomeric and elucidated the decay path to the $7/2^-$ ground state [13]. In this article, a significant extension to the level scheme for ^{163}W is reported with five new band structures observed.

II. EXPERIMENTAL DETAILS

The experiment was performed at the Accelerator Laboratory of the University of Jyväskylä, Finland. Excited states in ^{163}W were populated using the ^{106}Cd(^{60}Ni,2pn) reaction at a beam energy of 270 MeV. The target consisted of a 1.1 mg/cm^2 thick, self-supporting ^{106}Cd foil of 96.5% isotopic enrichment. An average beam current of 4 particle nA was

*Corresponding author: david.joss@liv.ac.uk

†Present address: Department of Physics, University of Guelph, Guelph, Ontario, N1G 2W1, Canada.

‡Present address: Instituut voor Kern- en Stralingfysica, Katholieke Universiteit Leuven, Celestijnenlaan 200D, B-3001 Leuven, Belgium.

§Present address: Department of Physics and Nuclear Engineering, Universitat Politècnica de Catalunya, Barcelona, Spain.

∥Present address: School of Engineering and Science, University of the West of Scotland, Paisley, United Kingdom.

¶Permanent address: UMR 8608, Université de Paris Sud/IN2P3, Division de Physique Théorique, Institut de Physique Nucléaire, 91406 Orsay Cedex, France.

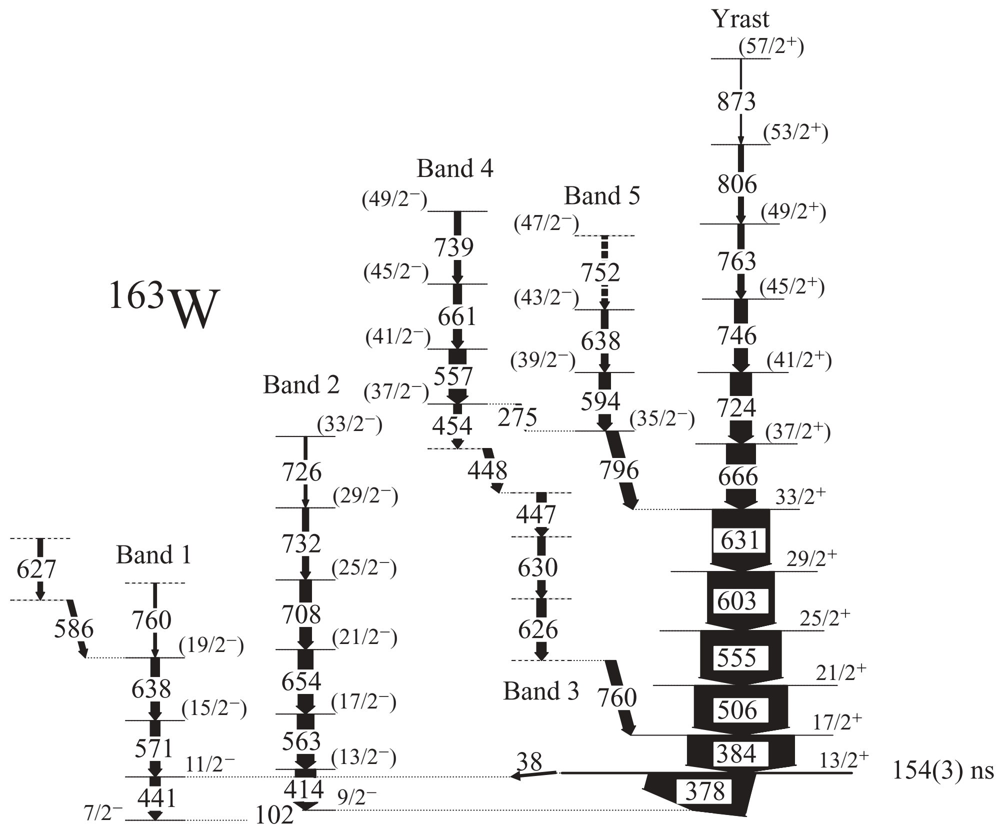

FIG. 1. Level scheme deduced for ^{163}W. The transition energies are given in keV and their relative intensities are proportional to the widths of the arrows. Dashed lines and parentheses indicate tentative assignments. The lifetime of the $13/2^+$ isomer is taken from Ref. [13].

used for five days. Prompt γ rays were recorded at the target position by the JUROGAM γ-ray spectrometer [14] consisting of 43 EUROGAM escape-suppressed germanium spectrometers [15].

The recoiling fusion-evaporation residues were separated from fission products and scattered beam by the RITU gas-filled recoil separator [16] and implanted into the double-sided silicon strip detectors (DSSDs) of the GREAT spectrometer [17] at the focal plane. Recoiling evaporation residues were distinguished from the residual scattered beam and radioactive decays by energy loss and (in conjunction with the DSSDs) time-of-flight methods using the GREAT multiwire proportional counter.

In addition to the planar and clover Ge detectors of the GREAT spectrometer, two VEGA clover detectors [18] were positioned perpendicular to the plane of implantation outside the GREAT vacuum chamber. All detector signals from JUROGAM and GREAT were passed to the total data readout acquisition system [19] where they were time stamped with a precision of 10 ns to allow accurate temporal correlations between γ rays detected at the target position, recoil implants at the focal plane, and their subsequent radioactive decays.

A. γ-ray coincidence analysis

A total of 1.18×10^8 three-fold (γ^3) events were recorded in coincidence with any recoil implanted at the focal plane. These data were sorted offline using the software package GRAIN [20] into an $E_{\gamma 1}$-$E_{\gamma 2}$-$E_{\gamma 3}$ coincidence cube, which was analyzed using the LEVIT8R graphical analysis software package [21]. The level scheme for ^{163}W was constructed using relative γ-ray intensities and coincidence relationships from spectra generated from this cube. The deduced level scheme for ^{163}W is displayed in Fig. 1 and the properties of γ rays in the yrast and newly observed bands are recorded in Table I.

B. Multipolarity assignments

Multipolarity assignments for the strongest γ-ray transitions were obtained from measurements of angular intensity ratios using the method of directional correlations from oriented states (DCO) [22]. Coincident γ rays observed in detectors at backward ($\theta = 158^\circ$) and normal ($\theta = 86^\circ$ or 94°) angles relative to the beam direction were sorted into a matrix. Multipolarities were extracted from intensity ratios according to the relation,

$$R_{\mathrm{DCO}} = \frac{I_{\mathrm{backward}}[\text{gated normal}]}{I_{\mathrm{normal}}[\text{gated backward}]}. \quad (1)$$

To obtain typical values for stretched quadrupole and stretched dipole transitions, the R_{DCO} value was measured for known stretched $E2$ and $E1$ transitions in ^{164}W that were populated strongly in this experiment and that were previously measured by Hanna [23]. The method employed clearly discriminated

TABLE I. Measured properties of γ-ray transitions detected by JUROGAM and assigned to ^{163}W. Energies are accurate to ±0.5 keV for the strong transitions ($I_\gamma > 10\%$) rising to ±2.0 keV for the weaker transitions.

E_γ (keV)	I_γ (%)	R_{DCO}	Multipolarity	Band
101.9	1.5(6)			2 → 1
275.1	4.0(5)			4 → 5
384.1	100.0(6)	0.79(12)	$E2$	Yrast
414.2	19(5)			1
441.3	10.0(26)			2
446.5	8.9(12)			3
448.4	8.0(10)			3
454.3	7.3(8)			3
506.2	89(9)	1.00(13)	$E2$	Yrast
554.6	77(7)	1.07(12)	$E2$	Yrast
556.7	16.3(18)			4
563.3	15.9(23)			2
571.4	9.2(16)			1
585.6	5.2(9)			1
594.1	10.8(13)			5
602.8	64(6)	1.19(13)	$E2$	Yrast
625.6	9.0(17)			3
627.1	4.6(14)			1
630.4	7.1(15)			3
631.1	55(5)	1.17(17)	$E2$	Yrast
637.6	8.2(13)			1
637.6	6.3(9)			5
654.3	14.4(20)			2
661.2	7.8(10)			4
666.3	28(3)			Yrast
708.0	13.0(15)			2
724.2	20.6(21)			Yrast
725.8	2.7(8)			2
732.0	6.0(9)			2
739.3	6.2(9)			4
746.3	12.5(14)			Yrast
752.5	5.5(8)			5
759.9	10.3(22)			3→ Yrast
760.3	2.6(8)			
762.8	5.9(9)			Yrast
796.0	11.5(14)			5 → Yrast
806.1	4.8(7)			Yrast
872.5	1.1(4)			Yrast

between stretched quadrupole and stretched dipole transitions, yielding R_{DCO} ratios of 0.94(9) and 0.67(14) for the 490 keV ($4^+ \rightarrow 2^+$) and the 752 keV ($7^- \rightarrow 6^+$) transitions in ^{164}W, respectively.

III. RESULTS

A. The yrast band, linked structures, and decay to the ground state

The yrast band, previously observed by Dracoulis *et al.* [12] up to $I^\pi = (49/2^+)$, has been extended to $(57/2^+)$. Figure 2(a) shows a sum of double-gated spectra highlighting transitions

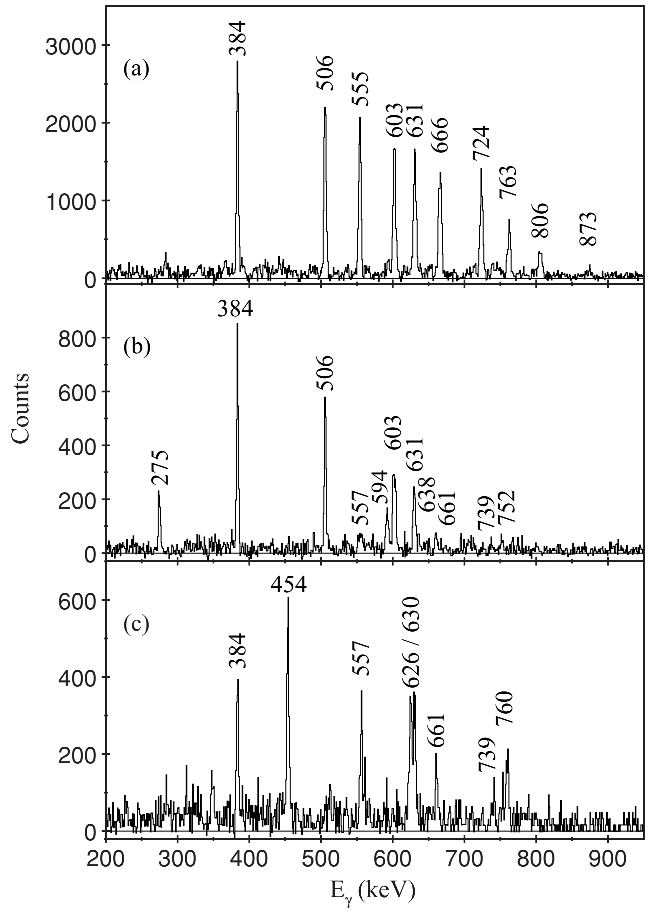

FIG. 2. (a) Double-gated γ-ray spectrum generated by summing coincidences between the 746 keV transition and a list of transitions comprising the 384, 506, 555, 603, 631, 666, and 724 keV transitions. (b) γ rays in coincidence with the 555 and 796 keV transitions showing transitions in bands feeding the yrast band. (c) γ rays in coincidence with the 446.5 and 448.4 keV transitions showing a parallel decay path from Band 4 to the low-spin states of the yrast band.

in the yrast band. In the present work it has been possible to establish three new band structures, labeled Bands 3, 4, and 5 in Fig. 1, that feed into the yrast band. Gamma-ray coincidences reveal the presence of a 796 keV γ ray that feeds the $33/2^+$ yrast state. A meaningful R_{DCO} value cannot be extracted for the 796 keV γ ray. Based on systematics of the heavier odd-N W isotopes [10,11], it is assumed that this transition is a stretched $E1$ transition connecting the yrast band to a negative-parity structure, labeled Band 5 in Fig. 1. Figure 2(b) shows γ rays in coincidence with the 796 and 555 keV transitions. The 275 keV γ ray, seen in Fig. 2(b), is found to be a linking transition to a parallel decay sequence labeled as Band 4 in Fig. 1. An R_{DCO} value cannot be obtained for this transition. However, again based on the systematics of similar structures in the heavier odd-N isotopes it is most likely to have negative parity.

Figure 2(c) shows γ rays in coincidence with both components of a self-coincident transitions at 446.5 and 448.4 keV. These transitions form part of an alternative decay path to the $17/2^+$ yrast state. Most of the transitions in this branch are assigned to the structure labeled Band 3. Since the 630 and 760 keV γ rays have similar energies to transitions in the yrast band it was not possible to order the transitions on the basis of relative intensities with any confidence. Consequently, Band 3 is indicated by tentative (dashed) levels in Fig. 1.

The decay path from the isomeric band head $13/2^+$ state to the $7/2^-$ ground state and the multipolarity of transitions between these states is discussed in detail by Scholey *et al.* [13] and is not discussed further in this article.

B. The ground-state band and first-excited band

The 441 keV transition, seen in the decay path from the isomer, is also the first transition of a band (labeled Band 1 in Fig. 1) that extends up to $(19/2^-)$. Figure 3(a) shows a double coincidence spectrum generated from the recoil-gated cube highlighting transitions in Band 1. Band 1 is weakly populated compared with the other bands and meaningful angular correlations cannot be extracted. Gamma-ray coincidences with the *M1* 102 keV γ ray reveal another regular cascade, Band 2, that extends up to $(33/2^-)$, see Figs. 3(b) and 3(c).

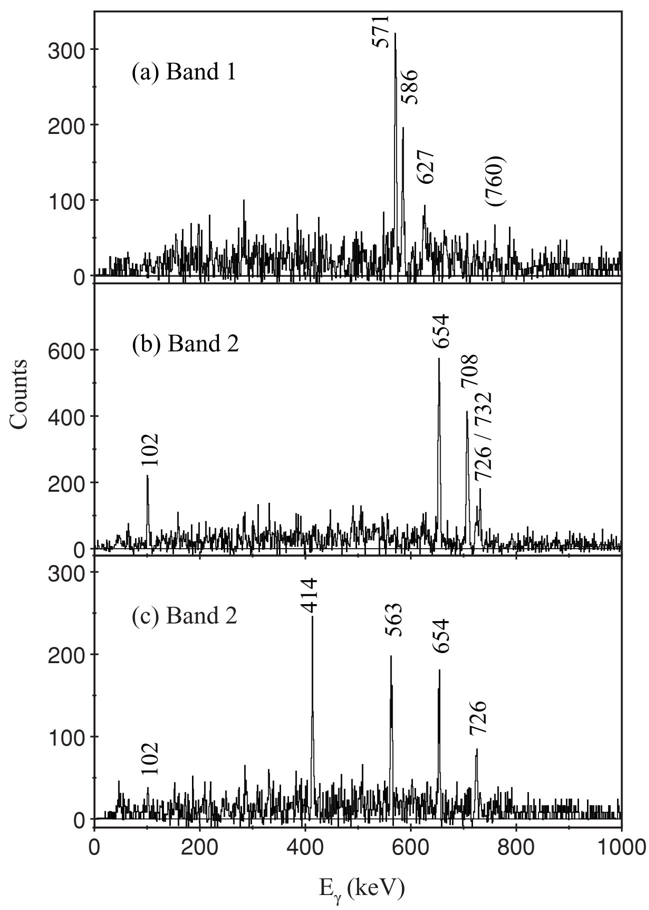

FIG. 3. (a) γ-ray spectrum showing γ rays in coincidence with the 441 and 638 keV transitions in Band 1. (b) γ-ray spectrum showing γ rays in coincidence with the 414 and 563 keV transitions in Band 2. (c) Spectrum showing γ rays in coincidence with the 708 and 732 keV transitions.

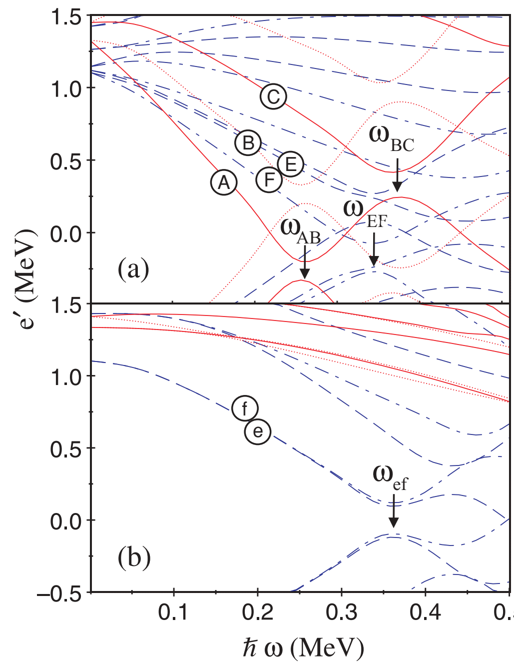

FIG. 4. (Color online) Cranked Woods-Saxon Routhian diagrams for (a) quasineutrons and (b) quasiprotons in ^{163}W using deformation parameters, $\beta_2 = 0.153$, $\beta_4 = 0.0$, and $\gamma = 0^\circ$. The quasiparticles are labeled with the convention as given in Table II. Solid lines correspond to $(\pi, \alpha) = (+,+1/2)$ (red), dotted lines $(+,-1/2)$ (red), dot-dashed lines $(-,+1/2)$ (blue), and dashed lines $(-,-1/2)$ (blue).

IV. DISCUSSION

The structure of the bands in ^{163}W is interpreted in terms of quasiparticle configurations within the framework Woods-Saxon cranking calculations using the Universal parameters [24,25]. Quasiparticle Routhians, e', calculated for ^{163}W are shown in Fig. 4. The labeling convention for quasiparticles, taken from Ref. [26], is given in Table II. In these calculations, the pairing strength is calculated at zero frequency and is modeled to decrease with increasing rotational frequency such that the pairing has fallen by 50% at $\hbar\omega = 0.70$ MeV, as detailed in Ref. [26]. Deformation parameters assume zero triaxiality, $\beta_4 = 0.0$ and the parameter $\beta_2 = 0.153$ is based on the predictions of Ref. [27].

TABLE II. Convention for the quasiparticle labeling, taken from Ref. [26].

Label	Parity & Signature (π,α)	Main Shell Model Component
	Quasineutrons	
A	$(+,+1/2)_1$	$i_{13/2}$
B	$(+,-1/2)_1$	$i_{13/2}$
C	$(+,+1/2)_2$	$i_{13/2}$
E	$(-,-1/2)_1$	$h_{9/2}$, $f_{7/2}$
F	$(-,+1/2)_1$	$h_{9/2}$, $f_{7/2}$
	Quasiprotons	
e	$(-,-1/2)_1$	$h_{11/2}$
f	$(-,+1/2)_1$	$h_{11/2}$

To facilitate comparisons between the calculations and results, experimental values for the Routhian e' and alignment i_x [28] as a function of rotational frequency are plotted in Fig. 5. A rotational reference, based on a configuration with a variable moment of inertia defined by the Harris parameters [29] $J_0 = 12.5\hbar^2$ MeV^{-1} and $J_1 = 60\hbar^4$ MeV^{-3} has been subtracted.

The Woods-Saxon cranking calculations, Fig. 4(a), indicate that the $i_{13/2}$ quasineutron A becomes the lowest in energy for rotational frequencies above $\hbar\omega = 0.1$ MeV. The yrast band of ^{163}W carries an initial alignment of $\sim 5\hbar$, see Fig. 5(a), which is consistent with the slope of the A Routhian ($i_x = -de'/d\omega$ [28]) predicted by the cranking calculations.

The yrast band in ^{163}W displays an alignment pattern that is markedly different from the yrast bands built on the $13/2^+$ state in the heavier odd-N isotopes ^{165}W [10] and ^{167}W [11], see Fig. 5(a). In these heavier isotopes, a single band crossing is observed and interpreted as the second $\nu(i_{13/2})^2$ BC neutron crossing [10,11]. In contrast, ^{163}W has two band crossings at $\hbar\omega \sim 0.30$ MeV and $\hbar\omega \sim 0.37$ MeV with corresponding alignment gains of $\Delta i_x \sim 6.5\hbar$ and $\Delta i_x \sim 6\hbar$, respectively.

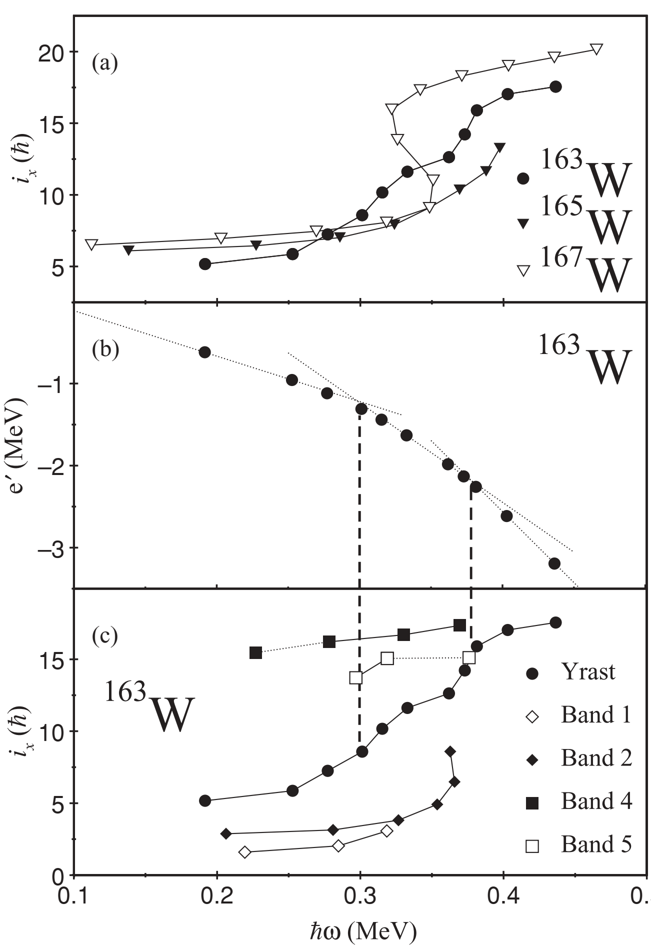

FIG. 5. (a) The alignment i_x as a function of rotational frequency for the yrast bands in the odd-N W isotopes, ^{163}W, ^{165}W [10], and ^{167}W [11]. (b) Experimental Routhians e' extracted for the yrast band in ^{163}W. The dotted lines indicate the slopes of the the Routhians used to extract crossing frequencies. Vertical dashed lines indicate the crossing frequencies that are interpreted as the EF and ef alignments. (c) Alignments i_x for the yrast band and Bands 1, 2, 4, and 5 in ^{163}W. The rotational reference subtracted is given in the text.

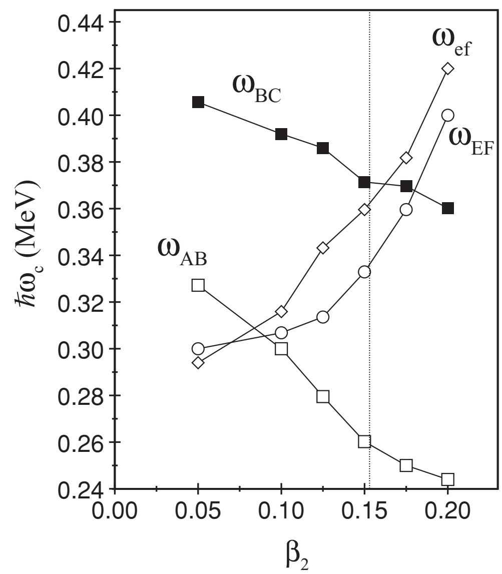

FIG. 6. (a) Variation of band crossing frequencies $\hbar\omega_c$ for different quasiparticle alignments (AB, BC, EF, and ef) as a function of quadrupole deformation parameter β_2. The $\hbar\omega_c$ values are predicted using Woods-Saxon cranking calculations. The dotted line indicates the β_2 deformation predicted by Ref. [27].

In the heavier odd-A isotopes the first band crossing in the yrast band is associated with the second $(i_{13/2})^2$ neutron alignment BC. However, for ^{163}W, which is predicted to have a lower deformation, the BC crossing is pushed to a higher rotational frequency. This can be seen in Fig. 4 where the yrast band is predicted to undergo the neutron $(h_{9/2}/f_{7/2})$ crossing EF closely followed by first $(h_{11/2})^2$ proton crossing ef. The calculations indicate that the crossing frequencies are all strongly dependent on the quadrupole deformation β_2. This is demonstrated in Fig. 6 where the band crossing frequencies $\hbar\omega_c$ are plotted as a function of β_2. In these calculations, β_4 and the triaxiality are set to zero and pairing is treated in the same manner outlined earlier. The cranked shell model predicts alignment gains of $\Delta i_x \sim 6\hbar$ for the EF alignment and $\Delta i_x \sim 8\hbar$ for the ef alignment. These values are similar to those measured in the experiment. The assignment of the EF crossing as the first alignment in the yrast sequence of ^{163}W is consistent with the assignment of an $(\nu h_{9/2})^2$ alignment in the yrast band in ^{162}W [12].

The properties of the γ rays depopulating the $13/2^+$ isomer in ^{163}W establish the spins and parities of the ground state and first-excited state to be $7/2^-$ and $9/2^-$, respectively [13]. These states are obtained by the odd neutron occupying the low-lying negative-parity orbitals. The cranked shell-model calculations, Fig. 4(a), predict that the mixed $h_{9/2}$ and $f_{7/2}$ negative-parity quasineutron states are lowest in energy at zero rotational frequency. Bands 1 and 2 are therefore interpreted as the single quasineutron configurations E and F, respectively. The larger alignment of Band 2 with respect to Band 1 is consistent with this interpretation. Band 2 has a gain in alignment at

TABLE III. Summary of configuration assignments for the bands in ^{163}W.

Band	(π,α)	Quasiparticle configuration assignment
Yrast	(+,+1/2)	$A \rightarrow AEF \rightarrow AEFef$
Band 1	(−,−1/2)	E
Band 2	(−,+1/2)	$F \rightarrow Fef$ or FAB
Band 4	(−,+1/2)	FAB
Band 5	(−,−1/2)	EAB

$\hbar\omega \sim 0.37$ MeV, see Fig. 5(c), which indicates a band crossing. Although the full alignment is not established the most likely interpretation is that it is the $\nu(i_{13/2})^2$ (AB) neutron alignment.

Bands 4 and 5 carry a higher alignment than the yrast band ($\sim 13\hbar$ at $\hbar\omega = 0.3$ MeV), which indicates that these bands are based on three-quasiparticle configurations, see Fig. 5(c). Bands 4 and 5 could be based on the FAB and EAB three-quasiparticle configurations. The larger alignment of Band 4 with respect to Band 5 is consistent with this interpretation. The alignment gain of the AB crossing is predicted by the Woods-Saxon calculations to be $\Delta i_x \sim 11\hbar$. The proposed configuration assignments and quasiparticle alignments that characterize the bands in ^{163}W are summarized in Table III. Band 3 is not included since the level ordering cannot be established and therefore its alignment is uncertain.

V. CONCLUSION

Five new band structures were observed in the neutron-deficient nucleus ^{163}W using the JUROGAM and GREAT spectrometers in conjunction with the RITU gas-filled separator. Configuration assignments for the new bands were proposed based on comparisons with the predictions of the Woods-Saxon cranked shell model. The irregular alignment pattern of the yrast band is attributed to the successive alignments of the negative-parity EF $(h_{9/2}, f_{7/2})$ quasineutrons and the ef $(h_{11/2})^2$ quasiprotons rather than the BC $(i_{13/2})^2$ quasineutron crossing as is observed in the heavier odd-A W isotopes. The favoring of negative-parity quasiparticle alignments for the $A \leqslant 163$ over the high-j $i_{13/2}$ quasineutrons is explained in terms of lower average deformations as the $N = 82$ shell closure is approached.

ACKNOWLEDGMENTS

Financial support for this work has been provided by the UK Science and Technology Facilities Council (STFC), the EU sixth Framework Programme,Integrating Infrastructure Initiative-Transnational Access, (EURONS, Contract No. 506065), the Academy of Finland under the Finnish Centre of Excellence Programme 2006–2011, and by the Swedish Research Council. P.T.G. (Contract No. 111965) and C.S. (Contract No. 209430) acknowledge the support of the Academy of Finland. We thank the UK/France (STFC/IN2P3) Loan Pool and the GAMMAPOOL European Spectroscopy Resource for the loan of detectors for JUROGAM and GSI for the loan of the VEGA detectors. The authors express their gratitude to the staff of the Accelerator Laboratory at the University of Jyväskylä for their excellent technical support. The authors also thank Paul Morrall of Daresbury Laboratory for preparation of the Cd targets.

[1] K.-H. Schmidt *et al.*, Phys. Lett. **B168**, 39 (1986).
[2] R. S. Simon *et al.*, Phys. Lett. **B325**, 197 (1986).
[3] E. S. Paul *et al.*, Phys. Rev. C **51**, 78 (1995).
[4] A. Keenan *et al.*, Phys. Rev. C **63**, 064309 (2001).
[5] D. T. Joss *et al.*, Phys. Rev. C **70**, 017302 (2004).
[6] M. B. Gómez Hornillos *et al.*, Phys. Rev. C **79**, 064314 (2009).
[7] D. O'Donnell *et al.*, Phys. Rev. C **79**, 051304(R) (2009).
[8] D. T. Joss *et al.*, J. Phys. G **31**, S1593 (2005).
[9] J. Simpson *et al.*, J. Phys. G **17**, 511 (1991).
[10] J. Simpson *et al.*, J. Phys. G **18**, 1207 (1992).
[11] K. Theine *et al.*, Nucl. Phys. **A548**, 71 (1992).
[12] G. D. Dracoulis *et al.*, Proceedings of the International Conference of Nuclear Structure at High Angular Momentum, Ottawa (1992), AECL Report No. 10613 (unpublished), Vol. 2, p. 94 and (private communication).
[13] C. Scholey *et al.*, Phys. Rev. C **81**, 014306 (2010).
[14] C. W. Beausang and J. Simpson, J. Phys. G **22**, 527 (1996).
[15] C. W. Beausang *et al.*, Nucl. Instrum. Methods Phys. Res. A **313**, 37 (1992).
[16] M. Leino *et al.*, Nucl. Instrum. Methods Phys. Res. B **99**, 653 (1995).
[17] R. D. Page *et al.*, Nucl. Instrum. Methods Phys. Res. B **204**, 634 (2003).
[18] J. Gerl, Nucl. Instrum. Method Phys. Res. A **442**, 238 (2000).
[19] I. H. Lazarus *et al.*, IEEE Trans. Nucl. Sci. **48**, 567 (2001).
[20] P. Rahkila, Nucl. Instrum. Methods Phys. Res. A **595**, 637 (2008).
[21] D. C. Radford, Nucl. Instrum. Methods Phys. Res. A **361**, 297 (1995).
[22] K. S. Krane, R. M. Steffen, and R. M. Wheeler, Nucl. Data Tables A **11**, 351 (1973).
[23] F. F. Hanna, Ph.D. Thesis, University of Liverpool (1993).
[24] W. Nazarewicz, J. Dudek, R. Bengtsson, and I. Ragnarsson, Nucl. Phys. **A435**, 397 (1985).
[25] S. Cwiok, J. Dudek, W. Nazarewicz, K. Skalski, and T. Werner, Comput. Phys. Commun. **46**, 379 (1987).
[26] R. Wyss, J. Nyberg, A. Johnson, R. Bengtsson, and W. Nazarewicz, Phys. Lett. **B215**, 211 (1988).
[27] P. Möller, J. R. Nix, W. D. Myers, and W. J. Swiatecki, At. Data Nucl. Data Tables **59**, 185 (1995).
[28] R. Bengtsson and S. Frauendorf, Nucl. Phys. **A327**, 139 (1979).
[29] S. M. Harris, Phys. Rev. **138**, B509 (1965).